Comparative Biochemistry and Physiology, Part B 224 (2018) 245–252

Contents lists available at ScienceDirect

Comparative Biochemistry and Physiology, Part B

journal homepage: www.elsevier.com/locate/cbpb

Increased transcript levels and kinetic function of pyruvate kinase during severe dehydration in aestivating African clawed frogs, *Xenopus laevis*

Neal J. Dawson*,[1], Yulia Biggar, Amal I. Malik, Kenneth B. Storey

Department of Biology and Institute of Biochemistry, Carleton University, Ottawa, ON, Canada

ARTICLE INFO

Keywords:
Allosteric regulation
Anaerobiosis
Gluconeogenesis
Glycolysis
Metabolism
Reversible protein phosphorylation

ABSTRACT

The African clawed frog, *Xenopus laevis*, can withstand extremely arid conditions through aestivation, resulting in dehydration and urea accumulation. Aestivating *X. laevis* reduce their metabolic rate, and rely on anaerobic glycolysis to meet reduced ATP demands. The present study investigated how severe dehydration affected the transcript levels, kinetic profile, and phosphorylation state of the key glycolytic enzyme pyruvate kinase (PK) in the liver and skeletal muscle of *X. laevis*. Compared to control frogs, severely dehydrated frogs showed an increase in the transcript abundance of both liver and muscle isoforms of PK. While the kinetics of muscle PK did not differ between dehydrated and control frogs, PK from the liver of dehydrated frogs had a lower K_m for phosphoenolpyruvate (PEP) (38%), a lower K_a for fructose-1,6-bisphosphate ($F1,6P_2$) (32%), and a greater activation of PK via $F1,6P_2$ (1.56-fold). PK from dehydrated frogs also had a lower phosphorylation-state (25%) in comparison to the enzyme from control frogs in the liver. Experimental manipulation of the phosphorylation-state of liver PK taken from control frogs by endogenous protein phosphatases resulted in decreased phosphorylation, and a similar kinetic profile as seen in dehydrated frogs. The physiological consequence of dehydration-induced PK modification appears to adjust PK function to remain active during a metabolically depressed state. This study provides evidence for the maintenance of PK activity through elevated mRNA levels and a dephosphorylation event which activates frog liver PK in the dehydrated state in order to facilitate the production of ATP via anaerobic glycolysis.

1. Introduction

The African clawed frog, *Xenopus laevis*, survives severe loss of aquatic habitat during arid periods. The seasonal drying and loss of water sources forces *X. laevis* to either migrate to find other aquatic habitats or burrow into the ground, entering a state termed aestivation. Aestivation is characterized by whole body water loss, urea accumulation, and entrance into a metabolically depressed state that can last for months (Hillman, 2009; Storey and Storey, 2004a, 2004b; Tinsley et al., 1996). During aestivation, *X. laevis* endures severe dehydration losing up to 35% of total body water (excluding bladder water) (Romspert, 1976). Some anurans (*Rana pipiens, Heleioporus eyrei*) can withstand daily fluctuations of > 22% of total body water (Dole, 1967; Lee, 1968). This remarkable tolerance to water loss is crucial for the survival of most anurans because the skin typically offers little resistance to evaporative water loss. In fact, the extent of dehydration endurance correlates strongly with the terrestrial nature of anuran habitats (Hillman, 1980; Joergensen, 1997; Thorson and Svihla, 1943; Thorson, 1955). Regulation of water balance to facilitate the endurance of dehydration involves a suite of behavioral, physiological, and biochemical responses (Churchill and Storey, 1993; Malik and Storey, 2009; Pinder et al., 1992). Dehydration-induced variability in body water content also leads to wide variations in body fluid osmolality and ionic strength and, among vertebrates, anurans show some of the greatest tolerance to variation in these parameters (Hillman, 1978, 1988, 2009). Another consequence of severe dehydration is reduced blood volume and increased blood viscosity which leads to impairment of aerobic cardiovascular capacity and performance, including a decline in arterial pressure, pulse rate, and oxygen consumption (Gatten Jr, 1987; Hillman, 1987). Due to decreased blood flow, tissues and organs can become hypoxic during severe dehydration, which induces an increased use of anaerobic energy production via glycolysis (Churchill and Storey, 1994a; Churchill and Storey, 1995; Hillman, 1978, 1987).

When aerobic energy production via oxidative phosphorylation is limited, such as in aestivating frogs, metabolic ATP production shifts from primarily oxidative phosphorylation to anaerobic production of ATP. Pyruvate, generated during glycolysis from the intermediate phosphoenolpyruvate, is converted to lactate under anaerobic

* Corresponding author at: McMaster University, Department of Biology, 1280 Main Street West, Hamilton, ON, Canada.
E-mail addresses: dawson1@mcmaster.ca (N.J. Dawson), neal.dawson@gmail.com (K.B. Storey).
[1] Present address: Department of Biology, McMaster University, Hamilton, ON, Canada.

https://doi.org/10.1016/j.cbpb.2018.01.003
Received 14 September 2017; Received in revised form 2 January 2018; Accepted 8 January 2018
Available online 10 January 2018
1096-4959/

conditions to regenerate the NAD^+ needed to sustain glycolysis. Pyruvate kinase (PK; E.C. 2.7.1.40) is responsible for catalyzing the following reaction:

phopshoenolpyruvate + ADP → pyruvate + ATP

This reaction is an important regulatory step in glycolysis, leading to production of pyruvate that can either be reduced (forming lactate) or oxidized (forming acetyl CoA), depending on conditions. In most cases, this reaction is essentially irreversible, representing one of the major points of control for glycolysis. Hence, mediation of PK activity is critical for regulating levels of ATP and glycolytic intermediates, while also serving as a metabolic control point, regulating the use of PEP by gluconeogenic or glycolytic pathways in tissues such as liver (Jurica et al., 1998; Mattevi et al., 1996; Valentini et al., 1995). Regulation of PK activity occurs via multiple mechanisms, including tight allosteric regulation and regulation via insulin-mediated cell signaling pathways (Jurica et al., 1998; Mattevi et al., 1996; Valentini et al., 1995). In this way, PK activity is responsive to the metabolic requirements of an organism, which may change depending on the energy state, tissue, or cell type.

PK has tissue specific isozymes, each of which exhibit different kinetic properties to meet the particular metabolic requirements of the expressing tissue. Although multiple PK isoforms can be detected in some tissues, cells generally express only one isoform at appreciable levels (Cardenas and Dyson, 1978; Imamura and Tanaka, 1972). The biochemical properties of the different PK isozymes are best characterized in mammals, which typically have four isozymes: PKL, which is the major isozyme in the liver and minor isozyme in the kidney; PKM1, which is associated with metabolically-demanding tissues like muscle, heart and brain; PKR, which is found exclusively in erythrocytes; and the embryonic PKM2, which is also found in proliferating cells (Cardenas and Dyson, 1978; Imamura and Tanaka, 1972; Imamura and Tanaka, 1982; Noguchi et al., 1986; Noguchi et al., 1987). The *pklr* gene encodes the liver and erythrocyte isozymes of PK (PKL, PKR), while the *pkm* gene encodes the two muscle isozymes (PKM1, PKM2) (Noguchi et al., 1986; Noguchi et al., 1987). In *X. laevis*, both *pklr* and *pkm* have been identified, but not all transcripts and isoforms have been characterized (Klein et al., 2002). Work so far suggests that the regulation of liver and muscle isozymes differs considerably. The muscle isozyme PKM1 is typically regarded as non-allosterically regulated, as it shows no responses to the binding of its inhibitors and/or activators under most conditions (Jurica et al., 1998); whereas, PKM2 is allosterically regulated (Israelsen and Vander Heiden, 2015). In contrast PKL, the liver isozyme is tightly regulated by the product of the phosphofructokinase 1 (PFK) reaction, fructose-1,6-bisphosphate ($F1,6P_2$) (Jurica et al., 1998). PKL is also allosterically regulated via feed-back inhibition by ATP, the product of the PK reaction, and by phosphorylation by cyclic AMP-dependent protein kinase (PKA) (Birnbaum and Fain, 1977; El-Maghrabi et al., 1982).

Aside for the action of inhibitors, activators and feedback loops, post-translational modifications, such as reversible protein phosphorylation, also play an important role in regulating key proteins in metabolic pathways in organisms that experience periods of dormancy (Dawson et al., 2013; Dawson et al., 2015; Dawson and Storey, 2011, 2012a, 2012b, 2016; Malik and Storey, 2009; Storey and Storey, 2004a). Post-translational modification of PK specifically has been reported in previous studies examining dormancy and metabolic rate depression in other animals such as the aestivating land snail (*Otala lactea*) and the freeze-tolerant goldenrod gall fly (*Eurosta solidaginis*) (Abboud, 2015; Whitwam and Storey, 1990). However, few studies have examined multiple isoforms, and no work to date has characterized the role of regulation of PK activity in aestivating frogs.

The purpose of this study is to understand the transcriptional, allosteric and post-translational regulation of pyruvate kinase under dehydration stress in *X. laevis*, which may facilitate increased glycolytic production of ATP in a metabolically depressed state. Here we report on the characterization of PK from hind limb muscle and liver of control and dehydrated *X. laevis* by investigating the differences in mRNA levels, enzyme kinetics, and post-translational modifications. In addition, we examine the effect of phosphorylation on the function of PK from control and dehydrated animals.

2. Materials and methods

2.1. Animals

African clawed frogs, *Xenopus laevis*, were donated from the Department of Zoology, University of Toronto. All animals were initially held in tanks of dechlorinated water, acclimated to 22 °C without food for at least 1 week. Animals were exposed to various levels of dehydration and were housed as described previously (Churchill and Storey, 1993). The frogs were divided into two groups; a control group (n = 4), and a severe dehydration group (> 25% body water lost) (n = 4). Control frogs were left in the tanks as previously described (Churchill and Storey, 1993). Dehydration groups were placed in closed containers and allowed to dry until ~25% of their body water was lost. To facilitate drying, a layer of silica gel desiccant was present in the container of the dehydration group; the silica gel desiccant was kept physically separate from the frogs using a perforated divider. Water loss was monitored for both groups over a period of 6–7 days by removing the animals at set intervals and weighing each animal. No significant changes in body mass were observed for the control groups. The change in body mass was used as a measurement of water loss using the following equation; % water lost = [(Wi − Wd) / (Wi × BWCi)] × 100, where Wi is the initial mass of the frog, Wd is the measured mass at each interval, and BWCi is the initial body water content of frogs prior to dehydration. For sampling, animals were killed by pithing and liver and hind limb skeletal muscle tissues were quickly harvested, immediately frozen in liquid nitrogen, and stored at −70 °C.

All experiments were conducted in accordance with the Canadian Council on Animal Care guidelines and The Carleton University Animal Care Committee.

2.2. Chemicals

Chemicals, biochemicals, chromatography media and coupling enzymes were from Sigma Chemical Co. (St. Louis, MO) whereas ProQ Diamond Phosphoprotein stain was from Invitrogen (Eugene, OR).

2.3. Preparation of tissue lysates for protein purification

Frozen liver and skeletal muscle samples were homogenized using a Polytron PT1000 homogenizer (1:5 w:v) on ice in buffer A (50 mM Tris, 25 mM NaF, 2.5 mM ethylenebis(oxyethylenenitrilo)tetraacetic (EGTA), 2.5 mM ethylenediaminetetraacetic acid (EDTA), 1 mM phenylmethylsulfonyl fluoride (PMSF), pH 8.0). PMSF crystals were added before homogenization process. Liver and skeletal muscle homogenates were centrifuged at 13500 × *g* at 4 °C for 20 min. The resulting supernatant was decanted and held on ice until use.

2.4. Sephadex G-50 and $DEAE^+$ chromatography of PK

A 5 cm column of Sephadex G-50 in a syringe barrel was equilibrated in buffer A and centrifuged at 500 × *g* in a bench-top centrifuge for 2 min to remove excess buffer. 500 µl aliquots of either liver or skeletal muscle extracts (1:5 w:v in buffer A) were centrifuge through the columns at 500 × *g* for 2 min. The resulting eluant was collected and 1 ml was applied to a $DEAE^+$ Sephadex G50 column (1.5 cm × 20 cm) equilibrated in buffer A, washed with 50 ml of buffer to remove unbound protein, and then eluted with a linear KCl gradient (0–1 M in 50 ml) in the same buffer. Fractions of ~0.6 ml were collected and 5 µl from each fraction was assayed to detect PK activity. The top 3 fractions

from the $DEAE^+$ Sephadex column were pooled.

2.5. Kinetic assays

PK activity was measured as the rate of pyruvate production coupled to an assay system using lactate dehydrogenase (LDH). Optimal assay conditions for PK were 50 mM Tris buffer pH 7.2, 50 mM KCl, 2.5 mM Mg·ADP, 5 mM phosphoenolpyruvate (PEP), 0.25 mM NADH, and 1 U/assay of LDH in a total volume of 200 µl with 5 µl of purified enzyme extract per assay. The kinetic parameters of muscle and liver PK were determined by varying the concentration of substrate or activations from zero to saturating levels. The concentrations used to determine the kinetic parameters for each substrate or activator are as follows (in mM): PEP (0, 0.025, 0.05, 0.075, 0.1, 0.3, 0.5, 0.75, 1, 1.5, 2), ADP (0, 0.025, 0.05, 0.075, 0.1, 0.3, 0.5, 0.75, 1, 3, 5), $F1,6P_2$ (0, 0.1, 0.2, 0.3, 0.4, 0.5, 0.75, 1, 2), AMP (0, 0.05, 0.1, 0.25, 0.5, 0.75, 1, 2). One unit of PK activity is defined as the amount of enzyme that consumed 1 µmol of PEP per minute at 25 °C. The amount of NADH consumed in the coupled reaction was measured at 340 nm with a Thermo Labsystems Multiskan spectrophotometer (Thermo Scientific, Waltham, MA, USA). Data were analyzed using the Kinetics v.3.5.1 program (Brooks, 1992). Protein concentrations were determined using the Coomassie blue dye-binding method with the BioRad prepared reagent and bovine serum albumin as the standard.

2.6. In vitro incubation to stimulate protein kinases and phosphatases

Samples of liver or skeletal muscle extracts, prepared as previously described in Section 2.3, were centrifuged through G50 Sephadex columns equilibrated in buffer B (50 mM Tris, 10% v:v glycerol, 30 mM β-mercaptoethanol, pH 8.0). Aliquots of the filtered supernatants were incubated for 12 h at ~4 °C with specific inhibitors and stimulators of protein kinases and phosphatases, as described in MacDonald and Storey (MacDonald and Storey, 1999). Each aliquot was mixed 1:2 v:v with the appropriate solutions in buffer B that were designed to stimulate protein phosphatases;

(I) STOP conditions: 2.5 mM EGTA, 2.5 mM EDTA and 30 mM β-glycerophosphate.
(II) Total phosphatase: 5 mM $MgCl_2$, 5 mM $CaCl_2$

After incubation, low molecular weight metabolites and ions were removed from the extracts by centrifugation for 2 min at 2000 ×*g* through small columns of Sephadex G50 equilibrated in buffer A before assay.

2.7. ProQ diamond phosphoprotein staining of liver isoform

PK was purified from liver tissue of both control and dehydrated frogs as described above. Aliquots of purified PK were then mixed 1:1 v:v with SDS loading buffer (100 mM Tris buffer, pH 6.8, 4% *w/v* SDS, 20% *v*/v glycerol, 0.2% w/v bromophenol blue, 10% v/v 2-mercapotethanol) and subsequently boiled for 5 min and stored at −20 °C until used. Equal volumes of each sample were loaded on a 10% SDS-PAGE gel together with PageRuler® pre-stained molecular weight standards (Thermo Scientific; Cat# 26616) and electrophoresis was carried out at 180 V for 45 min in running buffer (0.05 M Tris, 0.5 M glycine, 0.05% w/v SDS). The gel was removed and washed in fixing solution (50% v/v methanol, 10% v/v acetic acid) twice for 10 min, then left in fixing solution overnight at ~4 °C followed by 3 washes with ddH_2O for 10 min. The gel was then stained with ProQ Diamond Phosphoprotein stain for 30 min and washed. The gel was covered with aluminum foil during staining (and for the remainder of the protocol) to prevent the photosensitive stain from interacting with light. To minimize non-specific background, the gel was washed in ProQ Diamond destaining solution (20% v/v acetonitrile, 50 mM sodium acetate, pH 4) for 45 min, and then washed 3 times in ddH_20 for 10 min. The bands on the gel were visualized using the ChemiGenius Bioimaging System (Syngene, Frederick, MD) to assess the relative fluorescence intensities. The fluorescence of the bands was quantified using the accompanying GeneTools software.

2.8. Scansite prediction of phosphosites

In order to determine any potential phosphorylation sites of either muscle of liver PK, the Scansite application from the Massachusetts Institute of Technology (http://scansite.mit.edu/) was used to analyze the PK sequences from both muscle (NP_001080582) and liver (NP_001083514) of *X. laevis* in a search for putative phosphorylation sites.

2.9. Total RNA isolation

Total RNA was isolated from 100 mg of both liver and skeletal muscle. Each sample was homogenized using a Polytron homogenizer in 1 ml Trizol followed by the addition of 200 µl of chloroform and centrifugation at 10,000 ×*g* for 15 min at 4 °C. The upper aqueous layer (containing RNA) was removed and collected into a fresh microcentrifuge tube. Total RNA was then precipitated with the addition of 500 µl of isopropanol followed by incubation at room temperature for 10 min. The samples were placed in a centrifuge at 10,000 ×*g* for 10 min and the washed with 70% ethanol and centrifuged again. The RNA pellet was resuspended in 50 µl in DEPC-treated water. RNA quality was assessed by the 260/280 nm ratio and was confirmed by gel electrophoresis to check for integrity of the 18S and 28S ribosomal RNA bands.

2.10. Primer design

Primers were designed from *Xenopus laevis pklr* (NM_001090045.1) and *pkm* (NM_001090872.1) mRNA sequences downloaded from the NCBI gene database. Primer Designer program version 3.0 (Scientific and Educational Software) was used to design primers based on a number of different parameters obtained from IDT OligoAnalyzer 3.1 program (http://www.idtdna.com/analyzer/Applications/OligoAnalyzer/). Selected primer sets were chosen and purchased from Sigma Genosys; primers are listed in Table 1.

2.11. Reverse transcriptase-PCR

cDNA was prepared from a 5 µg aliquot of total RNA from each sample diluted to 10 µl with DEPC-treated H_2O and 1 µl of 200 ng/µl oligo-dT (5′-TTTTTTTTTTTTTTTTTTTTTTV-3′; V = A, G, or C) primer. Samples were incubated in a thermal cycler for 5 min at 65 °C, chilled on ice for 1 min and 4 µl of 5 × First strand buffer, 2 µl of 0.1 M dithiothreitol (DTT), 1 µl of 25 mM dNTPs (BioShop) and 1 µl of M-MLV reverse transcriptase (Invitrogen) were added to each sample. Samples were incubated for 45 min at 42 °C.

PCR was performed using a mixture of 15.5 µl of sterile water, 5 µl of diluted cDNA, 1.25 µl of primer mixture (to a final concentration of 1.5 µM forward and 1.5 µM reverse), 0.5 µl of 10× PCR buffer

Table 1
Sequences of primer pairs used in reverse transcriptase-PCR.

Gene	Primer	Primer sequence
pklr	Forward	5′ CACACCATTCGCAAGGAACT 3′
	Reverse	5′ ATACAGTCAGCTCCATCCAG 3′
pkm	Forward	5′ TCTGCGTGACTGAGATTGAG 3′
	Reverse	5′ TAAGCACGATGATGGCTCCA 3′
α-tubulin	Forward	5′ AAGGAAGATGCTGCCAATAA 3′
	Reverse	5′ GGTCACATTTCACCATCTG 3′

(Invitrogen), 1.5 µl $MgCl_2$ (50 mM), 0.5 µl of dNTP mixture (25 mM each) and 1 µl of *Taq* polymerase, for a total volume of 25 µl. All PCR amplification cycles were as follows; an initial denaturation at 94 °C for 7 min, followed by an optimized number of cycles of 94 °C for 1 min, primer annealing at 60 °C for 1 min, and elongation at 72 °C for 1 min. The final elongation was at 72 °C for 10 min. PCR products were separated on a 1% agarose gel, stained with 1 × Sybr Green I (Invitrogen). Band intensity was normalized against the corresponding intensity of α-tubulin bands amplified from the same RNA sample.

2.12. Statistical analysis

Data are presented as means ± SE. Student's *t*-tests (two-tailed; equality of variance was determined using F tests) were used to analyze enzyme kinetic parameters and relative protein phosphorylation levels. Analysis of post-incubation kinetics were performed using two-factor ANOVA followed by the Bonferroni post-tests to compare between dehydrated and control frogs within each incubation condition as well as incubation conditions within the control or dehydrated groups. $P < 0.05$ was considered significant.

3. Results

3.1. $DEAE^+$ purification of PK

The elution profile for *X. laevis* liver PK on a $DEAE^+$ ion exchange column is shown in Fig. 1. PK from control frogs eluted from the $DEAE^+$ ion exchange column yielding a peak at ~410 mM KCl (Fig. 1). However, PK from liver of dehydrated frogs eluted from the DEAE + ion exchange column much earlier at ~120 mM KCl (Fig. 1). There were no observable differences in the elution profiles for muscle PK from control and dehydrated frogs.

3.2. Kinetic characterization of PK

Kinetic parameters of liver PK, purified as described in Sections 2.4 and 2.5, were assessed to determine the differences in enzyme-substrate interactions between control and dehydrated forms. The K_m for PEP from the dehydrated form of PK decreased by 38% compared to PK from control frogs (Table 2; $p < 0.05$). The K_m value for ADP was not significantly different in the dehydrated form of PK in comparison to the control form (Table 2; $p > 0.05$). Additionally, there was no significant change in the V_{max} value for PK between the control and dehydrated forms (Table 2; $p > 0.05$).

In contrast to the kinetic parameters of the liver isoform, the kinetic parameters of the leg muscle form of PK resulted in no significant changes in kinetic parameters between the dehydrated state as compared to the control condition (Table 3 ; $p > 0.05$).

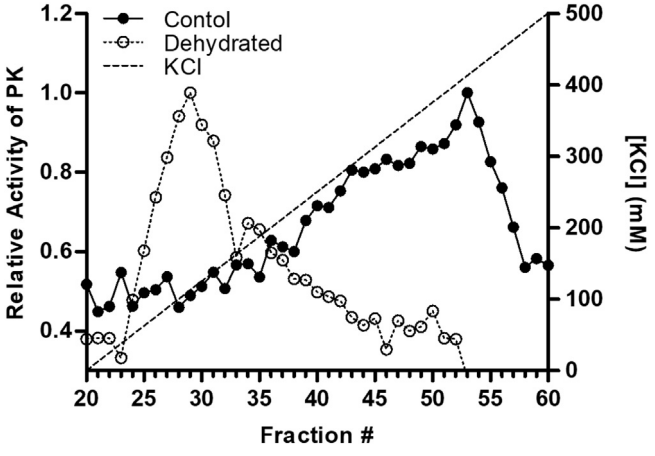

Fig. 1. Typical elution profile for PK from control and dehydrated liver on a $DEAE^+$ column. Solid line shows the KCl gradient use to elute PK from the column.

Table 2
The K_m for PEP and the Ka for F1,6P2 were significantly lower for PK from the liver of dehydrated *X. laevis* in comparison to control frogs. F1,6P2 also showed significantly greater activation of PK in the liver of dehydrated *X. laevis* in comparison to control frogs. PK was assayed in the PEP utilizing direction. K_m values were determined for crude enzyme extracts. Data are means ± SEM. * — Significantly different from the corresponding control value using Student's *t*-test, $p < 0.05$ (n = 4).

Enzyme parameter	Control	Dehydrated	F test
V_{max} (U/g wet weight)	38.1 ± 1.1	36.2 ± 1.8	$F_{3,3} = 2.678$, P = 0.4400
K_m PEP (mM)	0.29 ± 0.016	0.18 ± 0.015*	$F_{3,3} = 1.138$, P = 0.9180
K_m ADP (mM)	0.17 ± 0.018	0.18 ± 0.006	$F_{3,3} = 9.000$, P = 0.1041
I_{50} ATP (mM)	No effect (≤10)	No effect (≤10)	–
I_{50} Alanine (mM)	No effect (≤10)	No effect (≤10)	–
I_{50} Citrate (mM)	No effect (≤10)	No effect (≤10)	–
Ka $F1,6P_2$ (mM)	0.22 ± 0.009	0.15 ± 0.014*	$F_{3,3} = 2.420$, P = 0.4870
Fold activation	4.13 ± 0.35	6.44 ± 0.66*	$F_{3,3} = 3.556$, P = 0.3252
Ka AMP (mM)	0.64 ± 0.017	0.62 ± 0.028	$F_{3,3} = 2.713$, P = 0.4342
Fold activation	1.43 ± 0.028	1.35 ± 0.097	$F_{3,3} = 12.00$, P = 0.0707

Table 3
There were no significant differences in kinetic parameters for PK from the hind limb muscle of dehydrated and control *X. laevis*. PK was assayed in the PEP utilizing direction. K_m values were determined for crude enzyme extracts. Data are means ± SEM.

Enzyme parameter	Control	Dehydrated	F test
V_{max} (U/g wet weight)	94.8 ± 5.7	82.8 ± 3.6	$F_{3,3} = 2.507$, P = 0.4702
K_m PEP (mM)	0.19 ± 0.018	0.18 ± 0.025	$F_{3,3} = 1.929$, P = 0.6030
K_m ADP (mM)	1.26 ± 0.13	1.43 ± 0.12	$F_{3,3} = 1.174$, P = 0.8984
I_{50} ATP (mM)	No effect (≤10)	No effect (≤10)	–
I_{50} Alanine (mM)	No effect (≤10)	No effect (≤10)	–
I_{50} Citrate (mM)	No effect (≤10)	No effect (≤10)	–
Ka $F1,6P_2$ (mM)	0.38 ± 0.011	0.37 ± 0.014	$F_{3,3} = 1.620$, P = 0.7016
Fold Activation	3.16 ± 0.35	2.97 ± 0.66	$F_{3,3} = 3.556$, P = 0.3252
Ka AMP (mM)	0.74 ± 0.077	0.80 ± 0.068	$F_{3,3} = 1.282$, P = 0.8430
Fold Activation	1.33 ± 0.058	1.37 ± 0.099	$F_{3,3} = 2.913$, P = 0.4032

3.3. Effect of cellular metabolites on PK activity

The effects of cellular metabolites on the activity of *X. laevis* liver and skeletal muscle PK were evaluated (Tables 2, 3). In both the liver and skeletal muscle, the effects of the allosteric regulators ATP, alanine, citrate, fructose 1,6-bisphosphate ($F1,6P_2$) and AMP were explored. In both the liver and skeletal muscle, ATP, alanine and citrate had no effect on PK kinetic parameters at concentrations equal to or below 10 mM (Tables 2, 3; $p > 0.05$).

The K_a for $F1,6P_2$ was 220 µM for control liver PK, while a significant decrease (32%) in the K_a for $F1,6P_2$ under dehydration stress was observed (Table 2; $p < 0.05$). In addition, activation of PK activity by $F1,6P_2$ was significantly higher in the dehydrated form (6.44 fold-activation) in comparison to the control form (4.13 fold-activation) (Table 2; $p < 0.05$). AMP activated PK from both control and dehydrated animals; however no significant differences in the K_a or fold-activation were observed (Table 2; $p > 0.05$).

In the skeletal muscle, none of the tested metabolites showed differences between the control and dehydrated form (Table 3; $p > 0.05$). F1,6P_2 and AMP did activate skeletal muscle PK by ~3 and 1.3 fold respectively, whereas ATP, alanine, citrate did not elicit any significant changes in PK activity in concentrations equal to or < 10 mM (Table 3; $p > 0.05$).

3.4. Post-translational modification of endogenous PK

To test whether liver PK was modified by reversible phosphorylation, the peak fractions (based on activity) from the purification profiles for control and dehydrated frogs were combined and aliquots of enzyme were run on SDS-PAGE gels, and stained with ProQ Diamond phosphoprotein stain. When band densities were quantified, they showed a 1.3 fold higher band intensity for PK from liver of control frogs as compared to the enzyme from dehydrated frogs (Fig. 2; $p < 0.05$), indicating a higher content of bound phosphate on liver PK from control frogs.

3.5. In vitro post-translational modification of PK

To test whether or not reversible phosphorylation of PK could account for the observed changes in K_m for PEP that were seen between control and dehydrated states, incubations were set up such that crude extracts of liver were exposed to conditions that stimulated endogenous phosphatases. After incubation for 12 h at 4 °C, PK was purified as previously described in Section 2.4., and the effects of incubation on the K_m of PEP were measured.

The K_m of PEP was measured after incubations that promoted specific endogenous phosphates as described in Section 2.7. Stimulation of endogenous phosphatases resulted in a significant decrease in the K_m for PEP for PK from control frogs to a value not significantly different from the dehydrated form (Fig. 3; $p < 0.05$).

3.6. Scansite prediction of phosphosites

Analysis of PK sequences from both muscle (NP_001080582) and liver (NP_001083514) of *X. laevis* resulted in putative consensus sequences for phosphorylation sites on liver PK for ATM Kinase (threonine), Casein Kinase 1 (serine), Protein kinase A (PKA) (threonine), Protein kinase C (PKC) delta (serine), and PKC epsilon (serine); while the muscle form of PK was predicted to be phosphorylated by Casein Kinase 1 (serine), PKC alpha (threonine), PKC beta (threonine), PKC delta (serine), PKC gamma (threonine), PKC mu (serine) (Fig. 4). The protein sequence of muscle and liver PK from *X. laevis* showed a > 90% identity with *X. tropicalis*, but only ~50% identity with humans and other animals (UniProtKB; *pklr* Q6PA20_XENLA; *pkm* KPYM_XENLA).

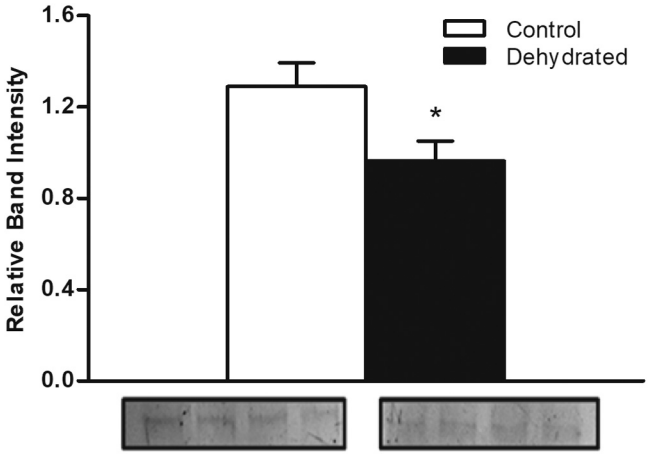

Fig. 2. PK purified from the liver of control *X. laevis* show significantly elevated levels of phosphorylation in comparison to dehydrated frogs with detection using ProQ Diamond phospho-protein stain. Data are mean ± SEM. * — Significantly different from the corresponding control value using Student's *t*-test, $p < 0.05$ ($n = 4$; $F_{3,3} = 1.094$, $P = 0.9428$).

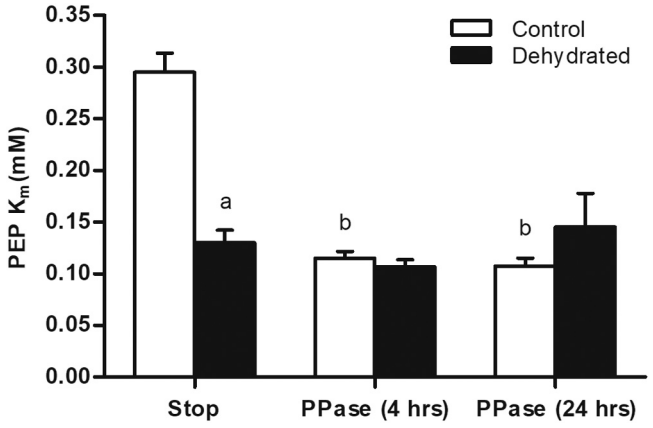

Fig. 3. The K_m value for PEP of purified liver PK was significantly decreased in control frogs after treatment with by in vitro incubations that stimulated the activities of endogenous protein phosphatases, but remained unchanged in dehydrated frogs. Data are mean ± SEM. There was a significant main effect of dehydration ($F_{1,18} = 10.77$, $P = 0.0041$), incubation ($F_{2,18} = 21.01$, $P < 0.0001$) and dehydration × incubation interaction ($F_{2,18} = 19.69$, $P < 0.0001$) ($n = 4$). a — Significant pairwise differences between the control and dehydrated frogs within the same incubation conditions in Bonferroni post-tests. b — Significant pairwise differences between the incubation conditions within control or dehydrated groups of frogs in Bonferroni post-tests.

3.7. mRNA levels of PK

Primers were designed based on the *X. laevis pklr* (NM_001090045.1) and *pkm* (NM_001090872.1) mRNA sequences downloaded from the NCBI gene database for use in relative quantitation of mRNA levels in the muscle and liver of control and dehydrated frogs. Alpha-tubulin was amplified from the same samples as a control. Transcript levels of *pklr* or *pkm* in dehydrated frogs look to be substantially higher in both the liver and hind limb muscle in comparison to control frogs (Fig. 5).

4. Discussion

Studies focused on long-term starvation in *X. laevis* show a reduction in oxygen consumption and key metabolic enzymes in the liver (LDH, glucose-6-phosphate dehydrogenase, PK) and muscle (LDH, PK) along with a nearly a complete depletion of liver glycogen reserves (Merkle, 1989; Merkle and Hanke, 1988). Metabolic adaptations supporting facultative anaerobiosis typically include: metabolic rate depression, access to reserves of a fermentable substrate, and substantial increases in the activities of glycolytic enzymes in all organs to facilitate anaerobic ATP production. Anaerobic glycolysis, the conversion of hexose phosphates to lactate, helps support the ATP requirements of the aestivating frog. As a result, there is a requirement for strict regulatory control over glycolytic rate, likely critical for the maintenance of energy homeostasis during long-term aestivation. Indeed, lactate levels in the dehydrating frog, *Pseudacris crucifer*, increased (5 fold) under dehydration conditions (Churchill and Storey, 1994a) and LDH function has been shown to be improved in *X. laevis* during dehydration through regulation by changes in urea levels in conjunction with post-translational modification (Katzenback et al., 2014). This increase in lactate has been attributed to hypoxia exposure, induced by a decrease in blood-flow as a result of increased blood viscosity in dehydrated animals, and is a strong indication of increase glycolytic activity (Hillman, 1978, 2009).

Pyruvate kinase is typically regulated tightly in accordance with the energy state or fed-state of the animal. In the fed state, PK is typically

A *Liver PK from X. laevis*

```
MAQLMQDLGP AFVQRQQLNA SMADTFLDHM CLLDIDSEPI TARNTSIVCT IGPASRSVEM  60
LKEMIKAGMN IARLNFSHGS HEYHAGSIHN IREATESFAS NPIHYRPVAI ALDTKGPEIR 120
TGVIKTGENT EVELMKGSIM KVTNDESFKD KCDEKILWVD YKNICKVVKV GGRIFVDDGL 180
ISLLVREIGP DYCMAEVENG GNLCSKKGVN LPGAPVDLPA LSERDCLDLK FGIEQGVDMV 240
FASFIRKAQD VHTIRKELGE KGRNIRIISK IENHEGVKRF DEILEASDGI MVARGDLGIE 300
IPAEKVFLAQ KMMIGRCNRA GKPVICATQM LESMIKKPRP TRAESSDVAN AVLDGADCIM 360
LSGETAKGLY PVESVHMQHA IAREAEAAIY NRQLFEELRR VTPLTQDPTE VTAIGAVEAS 420
FKCCAGAIIV LTTSGRSAQL LSRYRPRAPI IAVTRSAQVG RQAHLNRGVF PVLYQEAQLE 480
VWADDVDRRV QFAISIGKVR GFLSKDDIVI IVTGWRPGSG YTNIMQVVRV P          531
```

S(1): Casein Kinase 1
S(2): PKC delta, PKC epsilon
S(3): PKC delta
T(1): PKA
T(2): ATM Kinase

B *Muscle PK from X. laevis*

```
MSEAGSAFIQ TQQLHAAMAD TFLEHMCRLD IDSEPIVARN TGIICTIGPA SCSVEMLKEM  60
IKSGMNVARL NFSHGTHEYH AGTIKNVREA TESFASNPIH YRPVAVALDT KGPEIRTGLI 120
KGSGTAEVEL KKGATMRITL DDAFQEKCDE NVLWLDYKNL PKVVKPGSKI YVDDGLISLL 180
VKDIGPDFCV TEVENGGMLG SKKGVNLPGA AVDLPAVSPK DIQDLQFGVE QDVDMVFASF 240
IRKAADVHAV RKVLGEKGKN IKIISKIENH EGVRRFDEIL EASDGIMVAR GDLGIEIPAE 300
KVFLAQKMMI GRCNRAGKPI ICATQMLESM IKKPRPTRAE GSDVANAVLD GADCIMLSGE 360
TAKGDYPLEA VRMQHAIALE AEAAVFHRQL FEELFRATSS SRGPADAMAV GAVEASFKCL 420
ASAFIVMTES GRSAHLVSRY RPRAPIISVT RNGQTARQAH LYRGIFPVIY REAVHEAWAE 480
DVDRRVNFAM DIGKARGFFK SGDVVIVLTG WRPGSGFTNT MRVVPVP              527
```

S(1): Casein Kinase 1
S(2): PKC mu
S(3): PKC delta
T(1): PKC alpha, PKC beta, PKC gamma
T(2): PKC alpha, PKC beta, PKC gamma

Fig. 4. (A) The predicted phosphorylation sites for PK from the liver of *X. laevis*. (B) The predicted phosphorylation sites for PK from the muscle of *X. laevis*. Predicted phosphorylation sites are shown in bold and underlined. Kinases predicted to phosphorylate PK are listed below each sequence. Sequences were retrieved from the NCBI database with accession numbers NP_001080582 for muscle PK and NP_001083514 for liver PK.

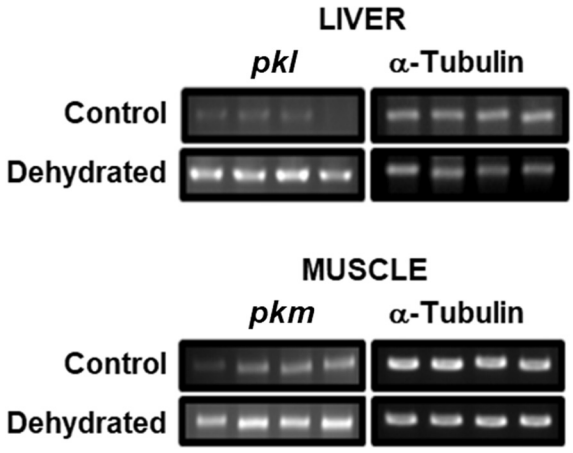

Fig. 5. PK transcript levels are higher in frog liver and muscle when compared using RT-PCR (n = 4).

dephosphorylated and active, allowing for the production of ATP from the newly acquired/digested glucose (El-Maghrabi et al., 1982). During a fasted-state, when food is scarce; pyruvate kinase is phosphorylated by PKA, inactivating it, preventing the conversion of PEP to pyruvate (El-Maghrabi et al., 1982). This allows the liver to preferentially produce glucose via gluconeogenic pathways for use by other tissues. Although one might be tempted to suggest that during prolonged dehydration *X. laevis* may mimic the fasted state, dehydration studies performed on the frogs, *Pseudacris crucifer* and *Rana sylvatica*, show that levels of glucose content initially rose dramatically in both the liver and muscle after dehydration (Churchill and Storey, 1994a; Churchill and Storey, 1994b). The authors suggested this rise in glucose levels may be due to a combination of increased gluconeogenic capacity in the liver and increased transport of glucose to the muscle (Churchill and Storey, 1994a; Churchill and Storey, 1994b). This suggests that dehydration in frogs may, in fact, be more analogous to the fed-state. Our results suggest that PK is indeed regulated in the liver of dehydrated *X. laevis*, which results in a low-phosphate, more active form of liver PK.

4.1. Kinetic changes of PK during severe dehydration

PK has tissue specific isoforms that are thought to be regulated in different manners: (1) the unregulated muscle PKM1 form which is constitutively active (Jurica et al., 1998), and (2) the tightly regulated liver (PKL) and muscle PKM2 isoforms which are controlled allosterically and via phosphorylation (Birnbaum and Fain, 1977; El-Maghrabi et al., 1982). The kinetic profiles for the muscle form of PK that we isolated did not show any differences between the control and dehydrated forms of PK (Table 3). Since we observed allosteric regulation via F1,6P_2, and AMP in muscle PK, it is highly likely that our purification yielded both PKM1 and PKM2 forms (Israelsen and Vander Heiden, 2015; Jurica et al., 1998).

In contrast to the muscle form, the K_m for PEP of liver PK significantly decreased in the dehydrated state as compared to the control state (Table 2) and is indicative of a higher affinity for PEP substrate during severe dehydration. Particularly in a situation of rising needs for non-oxidative sources of energy, increased affinity of PEP could

substantially increase the production of ATP via the glycolytic pathway. The dehydrated form of liver PK also showed an increased sensitivity to activation via F1,6P_2, suggesting a greater control of liver PK activity via allosteric effectors (Table 2). This is particularly interesting as levels of regulatory metabolites such as ATP have been shown to drop during the metabolically inactive state brought about by dehydration as energy stores are depleted in another dehydrating frog, *Pseudacris crucifer* (Churchill and Storey, 1994a). With prolonged dehydration exposure, liver ATP and total adenylates fell and changes in glycolytic intermediates were also consistent with an activation of glycolysis; concentrations of the PFK substrate F6P fell sharply, whereas those of the product F1,6P_2, increased (Churchill and Storey, 1994a). This is indicative of an activation of flux through the PFK locus. Furthermore, pyruvate also rose significantly in the liver suggesting a coordinated activation of PK, likely through allosteric activation via F1,6P_2 (Churchill and Storey, 1994a). Our results indicate that liver PK may indeed be more active during the dehydrated state as the affinity for both PEP and activation via F1,6P_2 were augmented, which, when combined with potentially increasing level of allosteric activators, would likely result in an increased anaerobic production of ATP.

4.2. Phosphorylation of PK

Investigation into further regulation of PK, it was discovered that the relative phosphorylation state of liver PK showed a significant difference in global phosphorylation levels (a 1.3 fold increase) of the enzyme in the dehydrated state as compared with the control state (Fig. 2). Interestingly, distinct peaks of liver PK activity were found when comparing the dehydrated form of PK to the control form during enzyme elution off a $DEAE^+$ column (Fig. 1). Previously, shifts to the right in elution profiles for proteins bound to a positively charged ion exchange column have been attributed to phosphorylation (or possibly other posttranslational modification) events, since the addition of phosphate groups adds a large negative charge to a protein (Abnous and Storey, 2008; Bell and Storey, 2010; Dawson and Storey, 2011, 2012a, 2012b, 2016; Holden and Storey, 2011; Lant and Storey, 2011). Hence, it is probable that the peak for the dehydrated form of liver PK eluting at lower salt concentration than the control form represents a low versus high phosphorylation states of the enzyme, respectively.

To further analyze liver PK posttranslational modification, enzyme preparations of the control animals were incubated under conditions that stimulated endogenous protein phosphatases. After subsequent purification, the protein phosphatase treated control-enzyme showed similar kinetic properties to those of the dehydrated form (Fig. 3). This adds strong support for the proposal that the difference in liver PK function found in dehydrated frogs is driven by a dephosphorylation event from high- versus low-phosphate forms of the enzyme and that dehydration stimulates the conversion of liver PK into a more active, low-phosphate form.

To test the viability of an alternate site for protein phosphorylation as a mechanism of PK control during dehydration, an investigation into the putative phosphorylation sites that might be present on PK was undertaken by analyzing the PK protein sequences of *X. laevis* (Fig. 4). This analysis showed the presence of putative PKA and PKC phosphorylation sites on *Xenopus* liver PK within well-conserved phosphorylation motifs for these two kinases. Putative phosphorylation sites were identified at threonine 402 for PKA and at serine 138 and serine 420 for PKC, supporting the idea that these PKA and/or PKC phosphorylation sites are highly likely to occur in *X. laevis* PK and are candidate sites for PK phosphorylation during dehydration. Since PKA is known to regulate PK in normal working conditions (Birnbaum and Fain, 1977; El-Maghrabi et al., 1982), it may fall upon alternate phosphorylation sites to help further regulate PK during dehydration, possibly through the activity of PKC. This may suggest that phosphorylation or dephosphorylation at alternate sites from the PKA regulatory site could result in an 'always on' state of the enzyme. During an energy-starved state, continually active PK would be required to continually produce ATP via glycolysis during a metabolically depressed state, despite the typical response by the liver to phosphorylate PK, inactivating it. This is of particular importance due to the fact that the liver is tasked primarily with producing glucose via gluconeogenesis, which could cause issues as blood flow is impaired during dehydration and a buildup of glucose may arise if left unchecked. Interestingly, there was no prediction of phosphorylation of PK from muscle via PKA, a known regulator of other PK isoforms (Fig. 4B) (Birnbaum and Fain, 1977; El-Maghrabi et al., 1982). This is in line with previous studies on the muscle form of PK which show little to no regulation, preferentially allowing glycolysis to run continually (Jurica et al., 1998; Mattevi et al., 1996; Valentini et al., 1995).

4.3. mRNA levels of PK

PK mRNA band intensities were greater in the liver and hind limb muscle of dehydrated *X. laevis* in comparison to control, which could suggest that PK transcript abundance may be elevated in the dehydrated state (Fig. 5). However, there was no difference when comparing individual enzyme maximal activity (Tables 1, 2). Elevated levels of PK transcripts could benefit the frog during dehydration by augmenting the capacity for PK synthesis to potentially offset protein degradation that may occur during prolonged dehydration, or, to sustain normal levels of PK synthesis despite global suppression of protein synthesis that accompanies metabolic rate depression (Storey and Storey, 2004a). There is some evidence that a shift from PKM1 to PKM2 expression occurs in cancer cells, resulting in an increased capacity for regulation (Mazurek, 2011), and while our results do not determine the relative amounts of each isoform, we do not see a change in the overall regulatory properties of the purified muscle PK which suggests that a shift in relative abundance of PKM1 versus PKM2 is unlikely. Nevertheless, it seems most likely that elevated mRNA levels of *pklr* and *pkm* aids *X. laevis* survive the dehydrated state by sustaining PK protein production counter to the global reduction in protein expression and/or in the face of dehydration-induced protein degradation to ensure sustained glycolytic ATP production.

5. Conclusion

Fine regulation of PK activity influences energy metabolism, and appears to be important in coping with dehydration in *X. laevis*. Pyruvate kinase from dehydrated frogs showed augmented kinetic function, likely due to a dephosphorylation event, and higher transcript abundance (which may offset the global reduction in protein synthesis associated with metabolic depression), when compared to control frogs. Augmented PK activity in the liver may increase the ability of *X. laevis* to control the rate of glycolysis via increased sensitivity to allosteric regulation and possibly increased anaerobic ATP production during the dehydrated state. Taken together, these modifications may aid in the preservation of pyruvate kinase activity, and by extension the function of the key energetic pathway of glycolysis, during dehydration

Acknowledgements

The authors thank J.M. Storey for assistance in editing this manuscript. This research was supported by a discovery grant from the Natural Sciences and Engineering Research Council of Canada (#6793) to KBS. NJD was supported by an Ontario Graduate Scholarship. Yulia Biggar was supported by a Canada Graduate Scholarship-Master's from the Natural Science and Engineering Research Council of Canada.

Conflict of interest

The authors declare no competing financial interests.

References

Abboud, J., 2015. Regulation of Pyruvate Kinase and Glycerol-3-phosphate Dehydrogenase in the Freeze Tolerant Goldenrod Gall Fly: Role in Polyol Cryoprotectant Production. Carleton University Ottawa.

Abnous, K., Storey, K.B., 2008. Skeletal muscle hexokinase: regulation in mammalian hibernation. Mol. Cell. Biochem. 319, 41–50.

Bell, R.A., Storey, K.B., 2010. Regulation of liver glutamate dehydrogenase by reversible phosphorylation in a hibernating mammal. Comp. Biochem. Physiol. B: Biochem. Mol. Biol. 157, 310–316.

Birnbaum, M.J., Fain, J.N., 1977. Activation of protein kinase and glycogen phosphorylase in isolated rat liver cells by glucagon and catecholamines. J. Biol. Chem. 252, 528–535.

Brooks, S., 1992. A simple computer program with statistical tests for the analysis of enzyme kinetics. BioTechniques 13, 906–911.

Cardenas, J.M., Dyson, R.D., 1978. Mammalian pyruvate kinase hybrid isozymes: tissue distribution and physiological significance. J. Exp. Zool. A Ecol. Genet. Physiol. 204, 361–367.

Churchill, T.A., Storey, K.B., 1993. Dehydration tolerance in wood frogs: a new perspective on development of amphibian freeze tolerance. Am. J. Phys. Regul. Integr. Comp. Phys. 265, R1324–R1332.

Churchill, T., Storey, K., 1994a. Effects of dehydration on organ metabolism in the frog pseudacris crucifer: hyperglycemic responses to dehydration mimic freezing-induced cryoprotectant production. J. Comp. Physiol. B. 164, 492–498.

Churchill, T.A., Storey, K.B., 1994b. Metabolic responses to dehydration by liver of the wood frog, *Rana sylvatica*. Can. J. Zool. 72, 1420–1425.

Churchill, T.A., Storey, K.B., 1995. Metabolic effects of dehydration on an aquatic frog, *Rana pipiens*. J. Exp. Biol. 198, 147–154.

Dawson, N.J., Storey, K.B., 2011. Regulation of tail muscle arginine kinase by reversible phosphorylation in an anoxia-tolerant crayfish. J. Comp. Physiol. B. 181, 851–859.

Dawson, N.J., Storey, K.B., 2012a. An enzymatic bridge between carbohydrate and amino acid metabolism: regulation of glutamate dehydrogenase by reversible phosphorylation in a severe hypoxia-tolerant crayfish. J. Comp. Physiol. B. 182, 331–340.

Dawson, N.J., Storey, K.B., 2012b. Regulation of tail muscle hexokinase in the anoxia-tolerant freshwater crayfish, *Orconectes virilis*. HOAJ Biol. 1 (1).

Dawson, N.J., Storey, K.B., 2016. A hydrogen peroxide safety valve: the reversible phosphorylation of catalase from the freeze-tolerant North American wood frog, *Rana sylvatica*. Biochim. Biophys. Acta Gen. Subj. 1860, 476–485.

Dawson, N.J., Bell, R.A., Storey, K.B., 2013. Purification and properties of white muscle lactate dehydrogenase from the anoxia-tolerant turtle, the red-eared slider, *Trachemys scripta elegans*. Enzym. Res. 2013.

Dawson, N.J., Katzenback, B.A., Storey, K.B., 2015. Free-radical first responders: the characterization of CuZnSOD and MnSOD regulation during freezing of the freeze-tolerant North American wood frog, *Rana sylvatica*. Biochim. Biophys. Acta Gen. Subj. 1850, 97–106.

Dole, J.W., 1967. The role of substrate moisture and dew in the water economy of leopard frogs, *Rana pipiens*. Copeia 141–149.

El-Maghrabi, M.R., Claus, T., McGrane, M., Pilkis, S., 1982. Influence of phosphorylation on the interaction of effectors with rat liver pyruvate kinase. J. Biol. Chem. 257, 233–240.

Gatten Jr, R.E., 1987. Activity metabolism of anuran amphibians: tolerance to dehydration. Physiol. Zool. 60, 576–585.

Hillman, S.S., 1978. The roles of oxygen delivery and electrolyte levels in the dehydrational death of *Xenopus laevis*. J. Comp. Physiol. A Neuroethol. Sens. Neural Behav. Physiol. 128, 169–175.

Hillman, S.S., 1980. Physiological correlates of differential dehydration tolerance in anuran amphibians. Copeia 125–129.

Hillman, S.S., 1987. Dehydrational effects on cardiovascular and metabolic capacity in two amphibians. Physiol. Zool. 60, 608–613.

Hillman, S.S., 1988. Dehydrational effects on brain and cerebrospinal fluid electrolytes in two amphibians. Physiol. Zool. 61, 254–259.

Hillman, S.S., 2009. Ecological and Environmental Physiology of Amphibians. Oxford University Press.

Holden, H.A., Storey, K.B., 2011. Reversible phosphorylation regulation of NADPH-linked polyol dehydrogenase in the freeze-avoiding gall moth, *Epiblema scudderiana*: role in glycerol metabolism. Arch. Insect Biochem. Physiol. 77, 32–44.

Imamura, K., Tanaka, T., 1972. Multimolecular forms of pyruvate kinase from rat and other mammalian tissues. J. Biochem. 71, 1043–1051.

Imamura, K., Tanaka, T., 1982. Pyruvate kinase isozymes from rat. Methods Enzymol. 90, 150–165.

Israelsen, W.J., Vander Heiden, M.G., 2015. Pyruvate kinase: function, regulation and role in cancer. Semin. Cell Dev. Biol. 43–51 Elsevier.

Joergensen, C.B., 1997. 200 years of amphibian water economy: from Robert Townson to the present. Biol. Rev. 72, 153–237.

Jurica, M.S., Mesecar, A., Heath, P.J., Shi, W., Nowak, T., Stoddard, B.L., 1998. The allosteric regulation of pyruvate kinase by fructose-1, 6-bisphosphate. Structure 6, 195–210.

Katzenback, B.A., Dawson, N.J., Storey, K.B., 2014. Purification and characterization of a urea sensitive lactate dehydrogenase from the liver of the African clawed frog, *Xenopus laevis*. J. Comp. Physiol. B. 184, 601–611.

Klein, S.L., Strausberg, R.L., Wagner, L., Pontius, J., Clifton, S.W., Richardson, P., 2002. Genetic and genomic tools for Xenopus research: the NIH Xenopus initiative. Dev. Dyn. 225, 384–391.

Lant, B., Storey, K.B., 2011. Glucose-6-phosphate dehydrogenase regulation in anoxia tolerance of the freshwater crayfish *Orconectes virilis*. Enzym. Res. 2011.

Lee, A.K., 1968. Water economy of the burrowing frog, *Heleioporus eyrei* (Gray). Copeia 741–745.

MacDonald, J.A., Storey, K.B., 1999. Regulation of ground squirrel Na+ K+-ATPase activity by reversible phosphorylation during hibernation. Biochem. Biophys. Res. Commun. 254, 424–429.

Malik, A.I., Storey, K.B., 2009. Activation of extracellular signal-regulated kinases during dehydration in the African clawed frog, *Xenopus laevis*. J. Exp. Biol. 212, 2595–2603.

Mattevi, A., Bolognesi, M., Valentini, G., 1996. The allosteric regulation of pyruvate kinase. FEBS Lett. 389, 15–19.

Mazurek, S., 2011. Pyruvate kinase type M2: a key regulator of the metabolic budget system in tumor cells. Int. J. Biochem. Cell Biol. 43, 969–980.

Merkle, S., 1989. Long-term starvation in *Xenopus laevis* Daudin—III. Effects on enzymes in several tissues. Comp. Biochem. Physiol. B 94, 783–788.

Merkle, S., Hanke, W., 1988. Long-term starvation in *Xenopus laevis* Daudin—II. Effects on several organs. Comp. Biochem. Physiol. A Physiol. 90, 491–495.

Noguchi, T., Inoue, H., Tanaka, T., 1986. The M1-and M2-type isozymes of rat pyruvate kinase are produced from the same gene by alternative RNA splicing. J. Biol. Chem. 261, 13807–13812.

Noguchi, T., Yamada, K., Inoue, H., Matsuda, T., Tanaka, T., 1987. The L-and R-type isozymes of rat pyruvate kinase are produced from a single gene by use of different promoters. J. Biol. Chem. 262, 14366–14371.

Pinder, A., Storey, K., Ultsch, G., 1992. Estivation and hibernation. Environ. Physiol. Amphibians 250–274.

Romspert, A.P., 1976. Osmoregulation of the African clawed frog. *Xenopus laevis*, in hypersaline media. Comp. Biochem. Physiol. A Physiol. 54, 207–210.

Storey, K.B., Storey, J.M., 2004a. Metabolic rate depression in animals: transcriptional and translational controls. Biol. Rev. 79, 207–233.

Storey, K.B., Storey, J.M., 2004b. Oxygen limitation and metabolic rate depression. Funct. Metab. Regul. Adapt. 415–442.

Thorson, T.B., 1955. The relationship of water economy to terrestrialism in amphibians. Ecology 36, 100–116.

Thorson, T., Svihla, A., 1943. Correlation of the habitats of amphibians with their ability to survive the loss of body water. Ecology 24, 374–381.

Tinsley, R.C., Loument, C., Kobel, H.R., 1996. Geographical distribution and ecology. In: Tinsley, R.C., Kobel, H.R. (Eds.), The biology of *Xenopus*. Oxford University Press, New York, pp. 35–60.

Valentini, G., Iadarola, P., Ferri, G., Speranza, M., 1995. Affinity labelling of the catalytic and allosteric ATP binding sites on pyruvate kinase type I from *Escherichia coli*. Biol. Chem. Hoppe Seyler 376, 231–235.

Whitwam, R.E., Storey, K.B., 1990. Pyruvate kinase from the land snail *Otala lactea*: regulation by reversible phosphorylation during estivation and anoxia. J. Exp. Biol. 154, 321–337.